24th INTERNATIONAL CONGRESS ON SOUND AND VIBRATION
23–27 July 2017, London

# CLASSIFICATION OF THE MID-FREQUENCY RANGE BASED ON SPATIAL FOURIER DECOMPOSITION OF OPERATIONAL DEFLECTION SHAPES

Jörn Biedermann, René Winter, Marco Norambuena and Marc Böswald
*Deutsches Zentrum für Luft und Raumfahrt (DLR), Institute of Aeroelasticity, Göttingen, Germany*
*email: joern.biedermann@dlr.de*

Martin Wandel
*AIRBUS Operations GmbH, Interior Noise Department, Hamburg, Germany*

Aircraft structures are characterized by their lightweight design. As such, they are prone to vibrations. On numerical side there are several tools suitable for the response analysis of dynamic structures. Each numerical tool is more adequate for different frequency ranges. The Finite Element Method, for example, is the state-of-the-art numerical tool for the low-frequency range where modal density is still low and methods based on the modal approach are still appropriate. For the high-frequency range, the Statistical Energy Analysis is more adequate. This method analyses the energy transmission between substructures and requires high modal density of the substructures. The intermediate section between low- and high-frequency is called the mid-frequency range and is characterized by strong interaction of vibrations and acoustics. The mid-frequency range typically suffers from a lack of tools available. Improvement of tools for the mid-frequency range is highly important e.g. for predicting the acoustic comfort inside an aircraft cabin, where interaction between vibrations and acoustics can be observed. However, as a prerequisite it is necessary to determine the beginning and the end of the mid-frequency range. This paper addresses a new method to be applied in acoustic comfort analysis of aircraft fuselage. It utilizes dynamic response measurements conducted on an aircraft fuselage, i.e. a stiffened cylindrical shell which exhibits global and local dynamic behaviour in the mid-frequency range. Existing criteria for the determination of the mid-frequency range are reviewed, but fail in this specific application. Therefore, a new method for the classification of the mid-frequency range for a stiffened cylindrical shell test-structure is proposed in this paper. It is based on wavenumber spectra obtained from spatial Fourier decomposition applied to operational deflection shapes extracted from experimental dynamic responses. Analysing the response characteristics of the different components of the aircraft fuselage a classification of frequency ranges is possible.

vibration analysis of the dynamic behaviour of lightweight aircraft structures, wavenumber analysis , mid-frequency range, high spatial resolution measurements

## 1. Introduction

Lightweight structures like an aircraft fuselage are designed for low mass and high stiffness. They are usually stiffened in longitudinal and circumferential direction to provide the necessary amount of structural stiffness. Such a design with discrete stiffeners (i.e. stingers in longitudinal and frames in circumferential direction) covered with a thin layer metal sheet (i.e. skin) shows a global structural dynamic behaviour in the low-frequency range with operational deflection shapes featuring structural

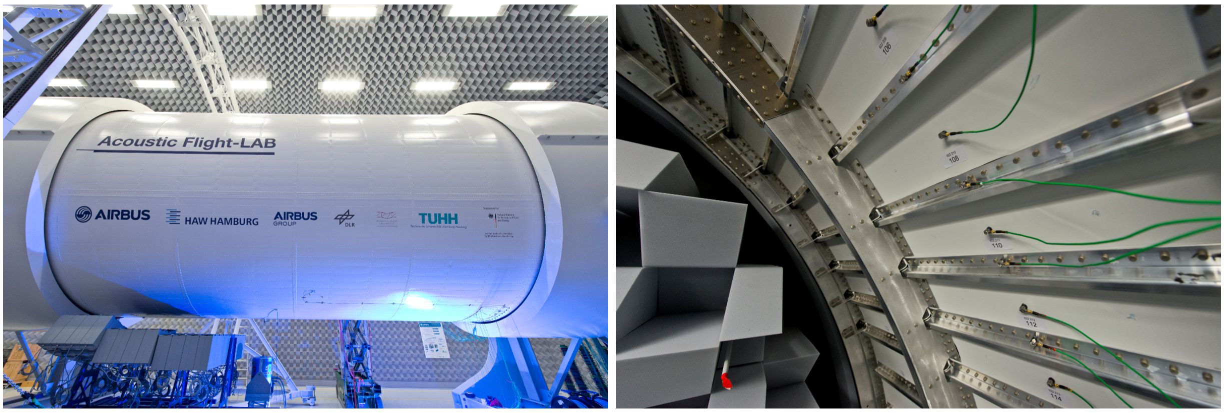


(a) (b)

Figure 1: (a) Acoustic FlightLAB demonstrator at ZAL in Hamburg. (b) Inside the demonstrator cabin showing frames, stringers, accelerometers and acoustic absorber.

waves extending over multiple neighbouring frames or stringers. The area framed between stringers and frames, covered by the thin layer of metal sheet, is called skin field. In the mid-frequency range a combination of global dynamic behaviour with superimposed strong local behaviour is present. In the high-frequency range an independent, dominant local behaviour of all structural components can be observed. This local behaviour can most efficiently be described in a statistical way because the accurate prediction of the exact vibration amplitudes of the skin fields is hard to achieve and also the prediction of the pattern of the vibration responses of multiple neighbouring skin fields. These features are highly sensitive to even small changes in the structural setup.

In [1, 2] the dynamic response of a vibroacoustic system in the low-, mid- and high-frequency range is described qualitatively. Based on the dynamic response of an ensemble of beams a frequency threshold for the low- and high-frequency range is presented in [3]. A common definition of the high-frequency threshold, which is often used in the Statistical Energy Analysis, can be obtained by the Modal Overlap Factor [4]. This qualifier is based on the modal density and structural damping, which are both hard to achieve from an experiment, especially beyond the low frequency range. Another way of defining the low-, mid- and high-frequency range is presented in [5] and is based on the ratio between the real and imaginary part of the input power, which is applied by a point force into a weakly coupled plate-structure.

A method is needed, which is independent from numerical data or estimations and works for weakly damped and stiffened lightweight structures, e.g. aircraft fuselage. Therefore, based on experimental results of a stiffened cylindrical test-structure, which is a generic model of an aircraft fuselage section, this paper proposes a method to divide the frequency range into the low-, mid- and high-frequency range. This classification is based on the structural wavenumbers of the operational deflection shapes, which are obtained with a 1D-Fourier Transformation of each operational deflection shape dominating a specific frequency of the dynamic response.

Furthermore, the interpretation of the individual dynamic behaviour of different components of an aircraft fuselage (frames, stringers and skin fields) is possible based on the structural wavenumbers.

## 2. Test-structure Acoustic FlightLAB demonstrator

The test-structure used in this paper is a generic aircraft fuselage, which is called 'Acoustic Flight-LAB'. The section of the aircraft fuselage demonstrator, which is installed in a dedicated suspension in a testing hall at the Zentrum für Angewandte Luftfahrtforschung (ZAL) in Hamburg, is about $8.5\,\mathrm{m}$ long and has a diameter of about $4\,\mathrm{m}$.

The fuselage demonstrator, which is shown in Fig. 1 (a), is mounted between two portals on

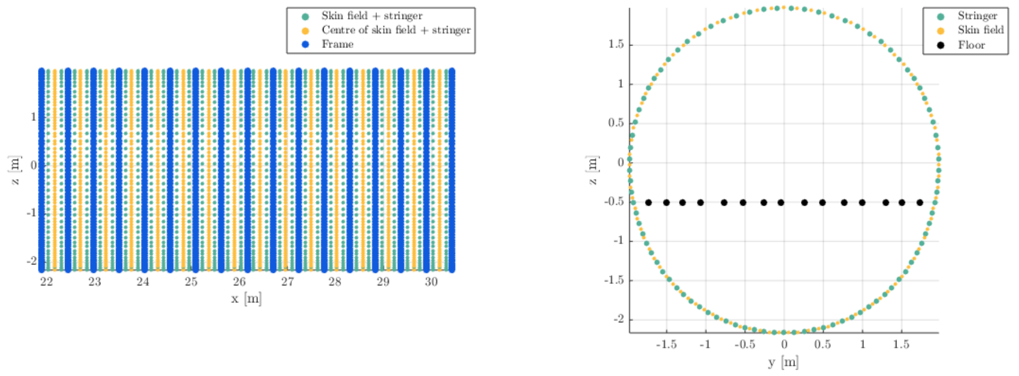


(a) (b)

Figure 2: (a) Sensor grid (xz-plane). (b) Sensor grid (yz-plane).

four nitrogen springs, which provide a soft suspension so that the vibrations of the demonstrator are fully decoupled from the environment. This test setup allows the fuselage to response almost unconstrained in radial direction on both ends. Both ends of the fuselage section are isolated with acoustic absorbers, which are necessary for acoustic measurements in the cabin cavity with known acoustic boundary conditions. These absorbers are shown in Fig. 1 (b). Figure 1 (b) also shows the underlying rip structure (17 frames and 87 stringers) of the fuselage and the accelerometers, which were used to measure the dynamic response of the fuselage due to a point force excitation. The electro-dynamic exciter, which provides the excitation, is radially attached under the fuselage to a stiff structural point, i.e. junction of frame and stringer, in order to distribute the excitation energy all over the structure, instead of vibrating just one skin field. In Fig. 1 (a) the exciter is placed in the middle of the fuselage.

The frequency range of interest was excited with a random signal, which is limited to the frequency range from $8\,\mathrm{Hz}$ to $1000\,\mathrm{Hz}$. This frequency range was chosen to cover the mid-frequency range, where the test-structure exhibits a global as well as strong local dynamic behaviour, which indicates that the excitation covers the low- and mid-frequency range.

For the dynamic tests on the FlighLAB fuselage a highly dense configuration of sensor positions is used because an accurate observation of local behaviour is only possible if the spatial resolution of the observation points is high enough. Figure 2 shows the sensor grid of the vibration tests, which were conducted in June 2016. In total, the dynamic response of the fuselage is measured on about 11310 points, including positions on the skin fields (yellow), frames (blue), stringers (green) and cabin floor (black).

## 3. Wavenumber analysis based on a 1D-Fourier Transformation

Wavenumber analysis is one of the tools to determine the mid-frequency range. It is performed by applying a 1D-Fourier Transformation ([6, p. 173]) on the operational deflection shapes. The objective is to characterize the dynamic response of different components of the structure at each measured frequency in order to split the whole measured frequency range into low-, mid- and high-frequency range. This classification gives a rough overview of the frequency range of validity for the different tools and methods.

The operational deflection shapes can be determined from response measurements, e.g. due to a harmonic point force excitation. The dynamic response $u$ of each measuring point can be transformed from the time domain into the frequency domain using a 1D-Fourier Transformation

$$\hat{u}(j\omega) = \mathcal{F}[u(t)] = \int_{-\infty}^{\infty} u(t)\, e^{-j\omega t} dt. \tag{1}$$

Arranging the transformed responses at frequency $\omega$ in a vector results in an operational deflection shape vector $\{\hat{u}(j\omega)\}$ at this specific frequency

$$\{u(t)\} = \Re\left(\{\hat{u}(j\omega)\}e^{-j\omega t}\right). \tag{2}$$

An exemplary operational deflection shape of the FlightLAB demonstrator at $96\,\mathrm{Hz}$ is shown in Fig. 3 (a).

Before applying a 1D-Fourier Transformation to the operational deflection shape, the 3D-cylinder is unwrapped onto a 2D-surface as shown in Fig. 3 (b). Considering only the radial component of the operational deflection shape, which is the most dominant degree of freedom for sound radiation into the cabin, enables a transformation into the wavenumber domain by applying a 1D-Fourier Transformation, which is shown in Fig. 3 (c). Figure 3 (c) shows in the upper diagram a slice of the deflection shape at $x = 26.16\,\mathrm{m}$ as a blue line and the resulting wavenumber spectrum $ky$ of this slice is illustrated in the lower diagram. The position of this slice is also marked in Fig. 3 (b) as a black dashed line.

The 1D-Fourier Transformation decomposes the operational deflection shape into a truncated series of fundamental waves with corresponding magnitude ($\{\hat{U}\}$) and wavenumber ($kx$,$ky$). In case of a cylinder $kx$ is the wavenumber in longitudinal and ky is the wavenumber in circumferential direction. A superposition of these fundamental waves results in the original operational deflection shape. For a discrete vibration pattern, e.g. in case of a discrete number of measuring points, a 1D-Fast-Fourier Transformation is most suitable and implemented in most numerical tools. An approximated solution of the original deflection shape gives the discrete superposition of N fundamental waves

$$u_y(x) = \Re\left(\sum_{r=1}^{N} \hat{U}_y(jkx_r)\, e^{-jkx_r\, x}\, \Delta kx\right), \tag{3}$$

$$u_x(y) = \Re\left(\sum_{r=1}^{N} \hat{U}_x(jky_r)\, e^{-jky_r\, y}\, \Delta ky\right). \tag{4}$$

$x$ and $y$ are coordinates of the unwrapped surface in Fig. 3 (b). In case of the wrapped cylinder $x$ is the coordinate in longitudinal direction and $y$ the coordinate along the circumferential direction.

The resulting operational deflection shape of the dominant wavenumber is plotted in the upper diagram of Fig. 3 (c) as a dark red, dashed line. The dominant wavenumber is the wavenumber, which contains the highest amount of vibration energy. It can be identified from the wavenumber spectrum as the highest peak. The highest peak is marked in the lower diagram of Fig. 3 (c) with a red dot.

After identifying the dominant wavenumber for all measured operational deflection shapes at all measured frequencies, a wavenumber-plot as a function of frequency and position can be arranged. The wavenumber-plot $ky$ for all measured $x$-positions and frequencies of the FlightLAB demonstrator is shown in Fig. 3 (d). The red, dashed line is the aliasing threshold of the measured sensor grid. In order to increase this threshold a higher resolution of measuring points is necessary. This process can also be repeated for the dominant wavenumbers $kx$ at all measured $y$-positions.

This wavenumber analysis is used later on to characterize and distinguish the measured frequency range into low-, mid- and high frequency range.

## 4. Wavenumber analysis of the FlightLAB demonstrator

Analysing the dominant wavenumbers of the FlightLAB demonstrator allows a characterization of the dynamic behaviour. A separation of the components (frames, stringers and skin fields) of the fuselage section is can be observed. Figure 4 (a) shows the wavenumber-plot $ky$ as a function of frequency and $x$-position and Fig. 4 (b) the wavenumber-plot $kx$. The wavenumbers $ky$ and $kx$ are represented as a colour-gradient.

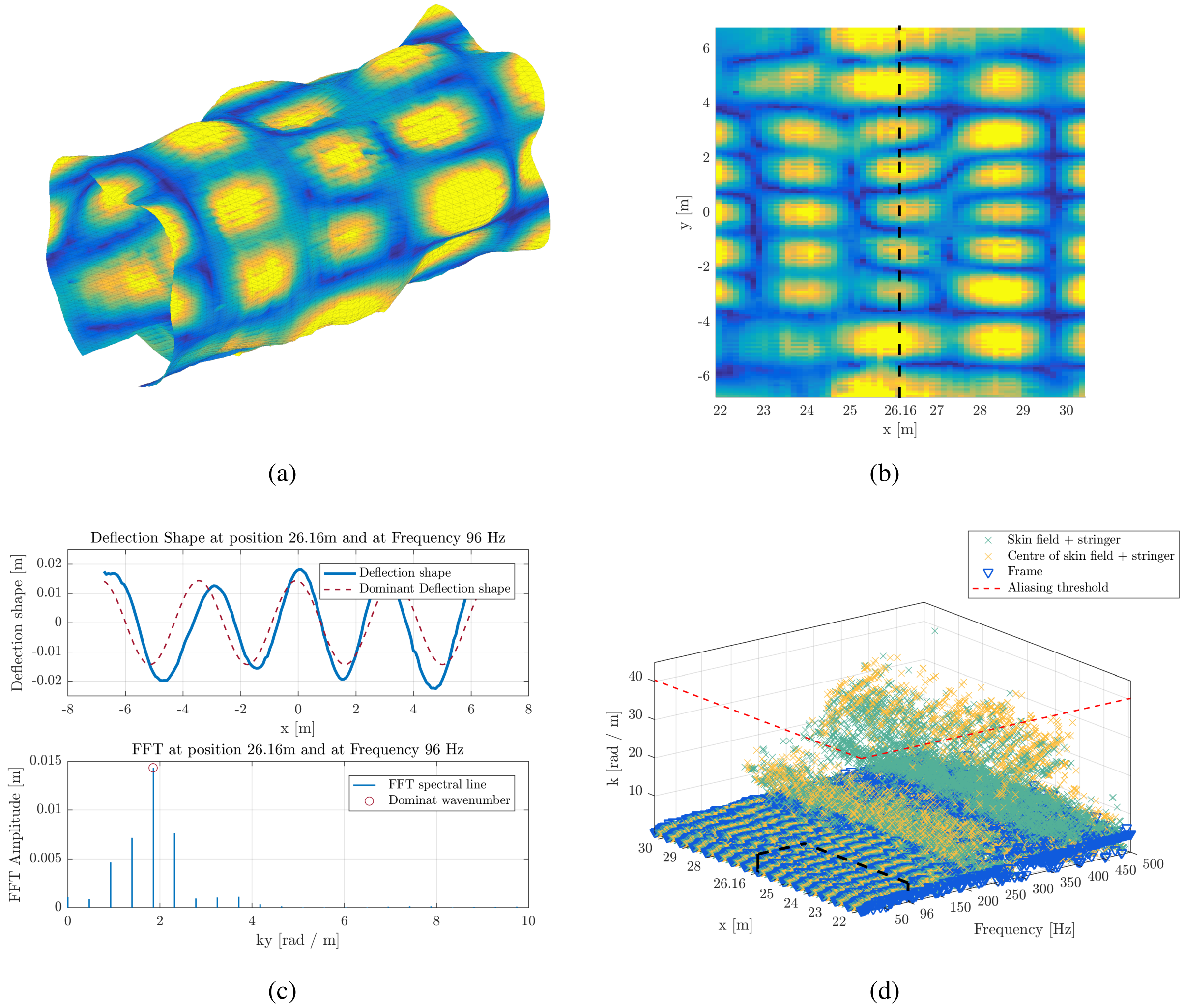


Figure 3: (a) Operational deflection shape at $96\,\mathrm{Hz}$. (b) Unwrapped Operational deflection shape onto a 2D-surface. (c) 1D-FFT applied to a slice of the operational deflection shape at $26.16\,\mathrm{m}$. (c) Dominant wavenumber $ky$ over x-position and frequency.

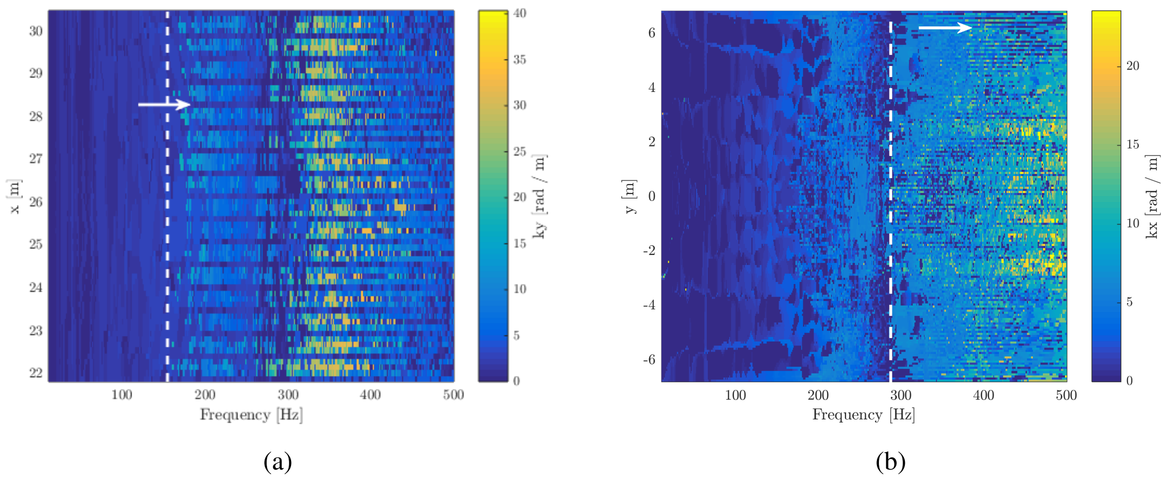


Figure 4: (a) Colour-gradient of the dominant wavenumber $ky$ as a function of $x$-position and frequency. (b) Colour-gradient of the dominant wavenumber $kx$ as a function of $y$-position and frequency.

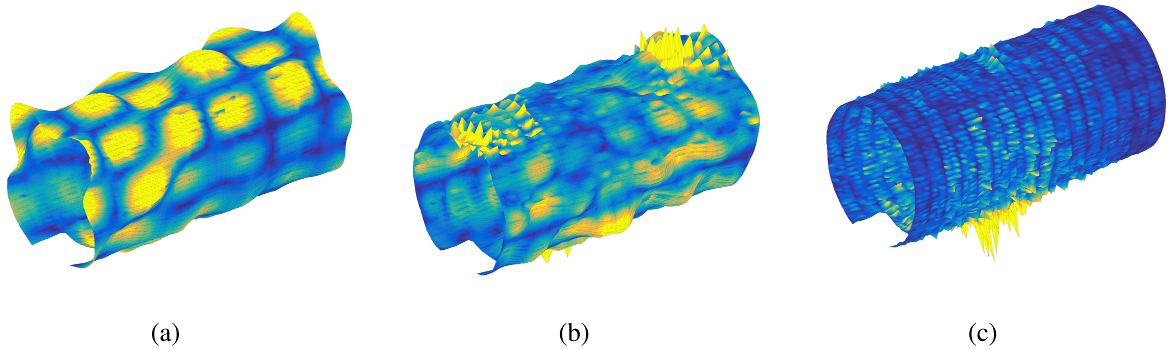


Figure 5: (a) Operational deflection shape at 118 Hz (**low-frequency range**). (b) Operational deflection shape at 163 Hz (**mid-frequency range**). (c) Operational deflection shape at 482 Hz (**high-frequency range**)

From Fig. 4 (a) a spatially correlated dynamic behaviour of all components of the fuselage section can be identified up to about 160 Hz (white, dashed line). All components along the $x$-axis exhibit similar wavenumbers in this frequency range. The $x$-position of the frames, stringers and skin fields are illustrated in Fig. 2 (a). Frames, stringers and skin fields show a similar dynamic behaviour, which results in a global deflection shape. The global behaviour of the fuselage section is illustrated in Fig. 5 (a) at 118 Hz.

Beyond 160 Hz straight vertical lines are clearly visible in the colour-gradient of Fig. 4 (a). These straight lines, which are marked exemplary for one line with a white arrow, correspond with the $x$-position of the frames. In this frequency range the dynamic behaviour of the frames seems spatially uncorrelated to the dynamic behaviour of the stringers and skin fields. In this frequency range the fuselage section exhibits a global as well as local dynamic behaviour. The local behaviour of the stringers and skin fields, which respond as a combined component, is superimposed to the global behaviour of the frames, which is shown in Fig. 5 (b) at 163 Hz. The local response of the stringers and skin fields is superimposed to the global response of the frames

Figure 4 (b) shows the wavenumber $kx$ as a function of frequency and $y$-position. The $y$-coordinates correspond to the unwrapped circumference of the cylinder shape of the fuselage. The corresponding components (stringers, skin fields) can be obtained from Fig. 2 (b). From Fig. 4 (b) a spatially correlated dynamic behaviour of all components of the fuselage section can be identified up to about 300 Hz (white, dashed line). Stringers and skin fields show a spatially correlated behaviour and respond in this frequency range as a combined component.

Beyond 300 Hz straight lines are again clearly visible in the colour-gradient. These straight lines, which are marked exemplary for one line with a white arrow, correspond with the $y$-position of the stringers. In this frequency range the dynamic behaviour of the stringers and skin fields seems spatially uncorrelated. Knowing from the wavenumber analysis $ky$ that also the frames show a spatially uncorrelated behaviour beyond 160 Hz, it can be concluded that all three components of the fuselage show a spatially uncorrelated dynamic response beyond 300 Hz. This spatially uncorrelated behaviour is illustrated in Fig. 5 (c), which shows the operational deflection shape at 482 Hz.

## 5. Classification of low-, mid- and high-frequency range

An interpretation of the dynamic behaviour of the different fuselage components, which is concluded from the wavenumber analyses, allows a classification of low-, mid- and high frequency range.

Up to 160 Hz the fuselage of the FlightLAB demonstrator exhibits a global dynamic behaviour due to a spatially correlated dynamic response of all three fuselage components. This frequency range is predestined for deterministic predictions, e.g. FEM, and for an Experimental Modal Analysis. Distinct resonance peaks in all Frequency Response Functions appear in this frequency range due to

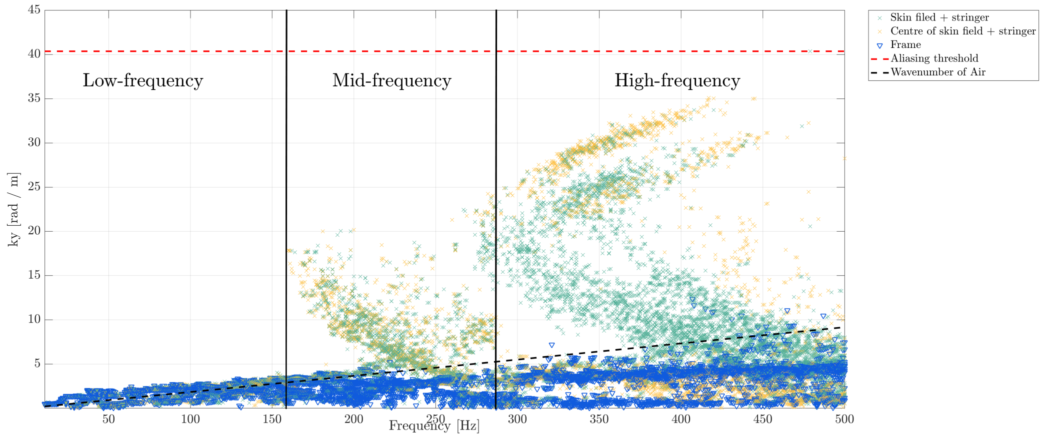


Figure 6: Classification of low-, mid- and high-frequency range.

the spatially correlated global behaviour. This behaviour defines the low-frequency range.

Beyond the low-frequency range up to 300 Hz the fuselage exhibits a global as well as local behaviour. The local resonances of the skin fields in this frequency range are more statistically distributed due to their low mass and stiffness compared to the frames. This behaviour is difficult to predict with deterministic methods and can be better characterized with statistical methods. This global and local behaviour is representative for the mid-frequency range and predestined for hybrid prediction methods, which include a deterministic as well as a statistical approach.

Beyond 300 Hz the dynamic behaviour of the fuselage seems rather local and irregular. All three components of the fuselage seem spatially uncorrelated, which recommends a statistical description of the dynamic behaviour of the fuselage. This pure statistical behaviour characterizes the high-frequency range and is predestined for statistical prediction methods, e.g. Statistical Energy Analysis. In addition, the strong local and spatially uncorrelated response behaviour indicates a high modal density and overlap.

Figure 6 shows the classification of low-, mid- and high-frequency range in the wavenumber-plot $ky$ over frequency. The separation of the wavenumbers beyond the low-frequency range is clearly visible. The wavenumbers of the frames (blue dots) separate from the stringers and skin fields (green and yellow dots).

In addition to the structural wavenumbers of the fuselage, Fig. 6 also shows the analytical wavenumber of air, i.e. the surrounding fluid of the demonstrator, as a function of frequency as a black dashed line. The analytical wavenumber of air is defined as $k_{air} = 2\pi\frac{f}{c}$ with the frequency $f$ and the speed of sound $c$. The speed of sound is estimated for this comparison with $c = 343\,\mathrm{ms}^{-1}$ under standard atmospheric conditions at sea level and $20\,°\mathrm{C}$.

Knowing that the sound radiation of the structure is less efficient if the structural wavenumber is larger than the wavenumber of surrounding air [7, p.462 ff.], the sound radiation of the fuselage of the FlightLAB demonstrator is dominated by the global dynamic behaviour of the frames and the local response of the skin fields, which is superimposed to the global response, is less important for acoustic assessments. Obviously, the sound is primarily radiated by the skin fields because they are physically coupled to the frames. However, the statistical distributed resonances of the individual skin fields, which are superimposed to the global behaviour of the frames, couple less strong with the cabin cavity. This information is important for the interpretation of acoustic measurements inside the cabin of the FlighLAB demonstrator.

**Note** The dominant wavenumbers at higher frequency are driven by the local resonances of individual skin fields. These resonances contain a high amount of energy and a separation from the global behaviour is possible. Obviously, all fuselage components are physically connected and the operational deflection shape is a superposition of the dynamic response of the frames, stringers and skin fields. Therefore, also the dynamic response of the frames can be identified with sensor positions on the skin fields alone if not only the dominant wavenumber is used for the analysis.

## 6. Conclusion

This paper proposes a new criterion for distinguishing the low-, mid- and high-frequency ranges for lightweight and stiffened cylindrical shell structures. For this criterion a high spatial resolution is required to identify the increasing wavenumbers with frequency.

Based on the global and local dynamic response of the fuselage demonstrator the low-, mid- and high-frequency range are determined by a wavenumber analysis on the operational deflection shapes. A 1D-Fourier-Transformation of the operational deflection shapes of each measured frequency is able to identify the frequency range at which the dynamic response of skin fields, stringer and frames tend to be spatially uncoupled.

A more global dynamic response is identified at lower frequency, which defines the low-frequency range. In this frequency range a prediction with deterministic methods is possible as well as an Experimental Modal Analysis because global and distinct resonances can be identified in this frequency range. At higher frequencies, skin fields, stringers and frames behave independent from each other. This spatially uncorrelated and irregular behaviour defines the high-frequency range. A prediction of this dynamic behaviour is only possible with statistical methods. In the mid-frequency range a mix of global as well local behaviour is present.

The proposed method is based a wavenumber analysis and is independent of numerical data or estimations. A qualitative classification of the frequency ranges is possible with experimental determined dynamic responses of weakly damped and flat structures, which are stiffened by an underlying rip structure. With this classification of frequency ranges suitable tools and methods for acoustic assessments or vibroacoustic predictions of aircraft structures can be selected.

## ACKNOWLEDGEMENTS

The experimental results of the Acoustic FlightLAB fuselage were conducted in the COCLEA project, which was funded by the German Federal Ministry for Economic Affairs and Energy (BMWi). The authors would like to express their gratitude to all people, who contributed to this project.

## REFERENCES

1. Soize, J.C., Desanti, A. and David, J.-M. Numerical methods in elastoacoustics for low and medium frequency ranges, *La Recherche Aérospatiale*, **5** (-), 25–44, (1992).

2. Ohayon, R. and Soize, C., *Structural Acoustics and Vibration: Mechanical Models, Variational Formulations and Discretization*, Academic Press, (1998).

3. Bernhard, R.J., Milner F.A. and Rabbiolo,G. Vibrations of a beam and related statistical properties, *Mathematical and Computer Modelling*, **34** (5), 657–675, (2001).

4. Rabbiolo, G. and Bernhard R.J. and Milner F.A. Definition of a high-frequency threshold for plates and acoustical spaces, *Journal of Sound and Vibration* , **277** (4-5), 647–667, (2004).

5. Okubo, N., Furuya, K., Toi, T., Seto, A. and Kanoko, S. Vibration energy control in mid frequency range based on principal component analysis, *Proceedings of International Conference on Noise and Vibration Engineering*, Katholieke Universiteit Leuven, Belgium, 2331–2340, (2014).

6. Brandt, A., *Noise and Vibration Analysis*, John Wiley & Sons, Ltd, (2011).

7. Cremer, L., Heckl, M. and Peterson, B.A.T., *Structure-Borne Sound*, Springer, Heidelberg, (2005).